International Journal on Recent and Innovation Trends in Computing and Communication
ISSN: 2321-8169 Volume: 11 Issue: 8
Article Received: *20 may 2023* ***Revised:*** *28 May 2023* ***Accepted:*** *16 August 2023*

Analysis of PFC Buck-Boost Converter Fed PMBLDC Motor Drive Systems

Martand Pratap, Dr. Shweta Singh,
Research Scholar, School of Engineering and Technology, MUIT, Lucknow

ABSTRACT

Electric motors influence almost every aspect of modern life. Refrigerators, vacuum cleaners, air conditioners, fans, computer hard drives, automatic vehicle windows, & a number of other household products & devices employ electric motors to convert electrical energy into usable mechanical energy. Electric motors power a wide range of industrial processes in addition to powering residential appliances. Brushless DC (BLDC) motor drives have grown in popularity in recent years due to their suitability for a wide range of low and medium power applications such as household appliances, medical equipment, position actuators, Heating, Ventilation, and Air Conditioning (HVAC), motion control, and transportation. These drives have great efficiency, dependability, durability, and outstanding performance across a wide range of speed control. The BLDC motor cannot be connected directly to the supply and must be driven by a drive consisting of VSI controlled by an electronic commutation system. Harmonics are introduced into the main power supply and power factor issue by the electronic commutation system and rectification procedure. Power Factor Correction (PFC) converters are used to improve the power quality and power factor of the alternating current mains.

Keywords: Buck-Boost Converter, Power Factor Correction (PFC), PMBLDC, Motor Drive System etc.

INTRODUCTION

Throughout past decade, electric drives have been employed in a variety of applications including industrial, household appliances, medical equipment, and the automobile industry. Machine tools, industrial robots, automated presses, conveyors, elevators, rolling mills, pumps, fans, compressors, electrical vehicles, cranes, the textile sector, and many more uses consume more than two-thirds of all electric energy generated in an industrialised nation. Complicated process and motor control activities are carried out with the assistance of high throughput digital controllers and sub tiny signal processors capable of completing operations per second. An increase in PWM frequency allows the current and torque control loops to respond faster, improving overall drive performance.

An electric motor is a device that transforms electrical energy into mechanical energy. An electric motor may also move energy from a power source to a mechanical load. The drive, also known as the electric drive or motor drive, is the mechanism that houses and spins the motor. The motor drive's job is to harvest electrical energy from an electrical source & supply it to motor in order to generate required mechanical output. This is also known as motor's speed, torque, & shaft position.

The advancement of strong digital microcontrollers enables full-digital control of electromechanical adaption processes in an electrical drive. Automation made great advances in this process in the 1950s, owing to the development of Numerical Control (NC). While neither flexible or entirely programmable, NC systems have mostly replaced the mechanical timers that were ubiquitous in the industry in the early part of the twentieth century. Because the first dependable and commercially accessible microcontrollers were developed in the 1960s, they were widely employed for the flexible control of electric drives in low-power applications.

Electric motors have an impact on practically every element of modern life. Electric motors are used in refrigerators, vacuum cleaners, elevators, air conditioners, washing machines, fans, computer hard disc drives, & industrial operations. In reality, motors consume majority of energy, regardless of whether application is domestic, industrial, or commercial. The energy percent efficiency of a motor is determined by its kind. Some are designed to be more energy efficient than others. In addition, the recent fast growth of motor drives in vehicle sector with the introduction of new hybrid technologies has produced a significant need for highly efficient variable speed motor drives.

In general, three types of tasks must be completed: beginning, speed governor, and braking, all of which are mostly accomplished by electrical motors. As a result, it

International Journal on Recent and Innovation Trends in Computing and Communication
ISSN: 2321-8169 Volume: 11 Issue: 8
Article Received: *20 may 2023* ***Revised:*** *28 May 2023* ***Accepted:*** *16 August 2023*

attests to the supremacy of motor in all aspects. Control and monitoring of various parameters using a variety of approaches are required for overall drive control (Leonhard W (2001) (Crowder R. (2006).

There are two types of control structures: open loop & closed loop control systems. In an open loop governing network, response has no effect on source, implying that controlling event is self-governing of output. The closed loop system is more better & methodical. At this point, productivity is returned to contribution terminal, which determines amount of input to system.

CLOSED LOOP CURRENT LIMIT GOVERNOR

Fig.1 depicts the current limit control block diagram. It is examined to ensure that preventive estimations are not overlooked. As a result, there is a possibility of huge current flows across motor route. The current frontier percent controller is located in order to connect current and perception of percent current to a motor. The feedback percent loop has no effect on regular driving performance. But, if current exceeds the predetermined limit, feedback loop is activated, causing the current to fall below the safe level.

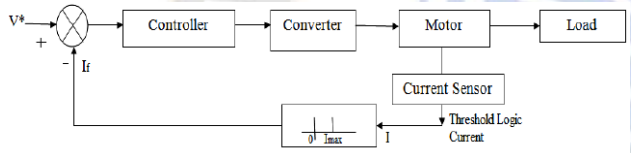

FIG. 1: CURRENT LIMIT GOVERNOR

CLOSED LOOP TORQUE GOVERNOR

This sort of torque percent regulator is commonly used in battery-powered vehicles such as trains and automobiles. The operator compacts accelerator in the car to locate the indicated torque 'T'. As shown in Fig. 2, actual torque T exceeds prescribed torque T*, which is disallowed by operator through accelerator.

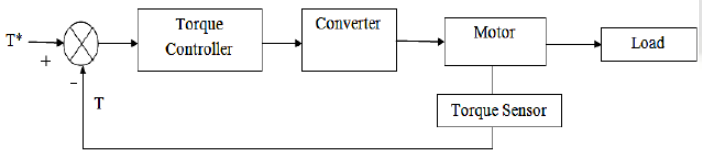

FIG. 2: CLOSED LOOP TORQUE GOVERNOR

CLOSED LOOP SPEED GOVERNOR

Speed control loops are most likely employed as drive feedback loops. Fig. 3 depicts a closed loop speed governor. Internal and outside loops are the two capable control loops. The inner control loop keeps converter & motor current or torque within safe limits. Now we can read control loop portion & drive with appropriate examples. Assuming indicated speed m* increases & a constructive error m is produced, indicating that the momentum must be improved.

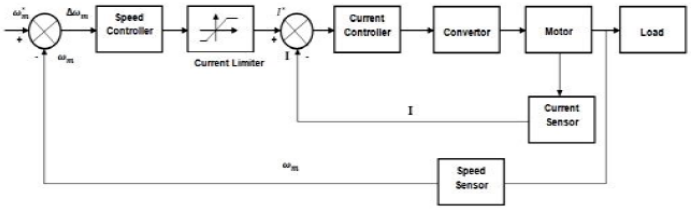

FIG. 3: CLOSED LOOP SPEED GOVERNOR

The internal loop will now keep it below the maximum allowable current. The motorist then accelerates. As a result, throughout speed control, the purpose passes from driving to braking and back again, subjecting the motor to heat and sprinting. Loop closure Control methods are more expensive economically, can improve by reducing loss, and occasionally feedback causes the system to oscillate, resulting in an oscillating response. Vector control is favoured to compensate for all of these limitations since it has good speed regulation, achieves maximum torque at zero speed, is highly responsive, easy to modify, & has a better level of safety.

POWER FACTOR CORRECTION

Power factor is most important metric in power electronics since it indicates how effective the system's real power use is. It also represents a measure of line voltage & current distortion, as well as the phase shift between them. In an alternating current circuit, Power Factor (PF) is defined as ratio of real power to apparent power, as shown in Eq. 1. Nevertheless, due to non-linear behaviour of active switching power devices in power electronic systems, phase-angle description alone is not acceptable. The non-linear load draws typical distorted line current from line, as shown in Figure 4(a).

$$\text{Power factor} = \frac{Real\ Power\ (P)}{Apparent\ Power\ (S)} = \frac{P}{VI} \quad (1)$$

When the load in a linear system draws entirely sinusoidal current & voltage, PF becomes cosine of phase angle b/w current & voltage, as shown in eq. 2.

$$\text{Power factor} = \frac{\text{Vrms Irms Cos}\phi}{\text{Vrms Irms}} = \text{Cos}\phi \quad (2)$$

International Journal on Recent and Innovation Trends in Computing and Communication
ISSN: 2321-8169 Volume: 11 Issue: 8
Article Received: *20 may 2023* ***Revised:*** *28 May 2023* ***Accepted:*** *16 August 2023*

$$I = \frac{P}{V \cos\phi}$$

(3)

Calculating PF for distorted waveforms is more difficult than for sinusoidal waveforms. The power factor is enhanced by lowering reactive power & decreasing the power factor angle, as illustrated in Fig. 4. (b).

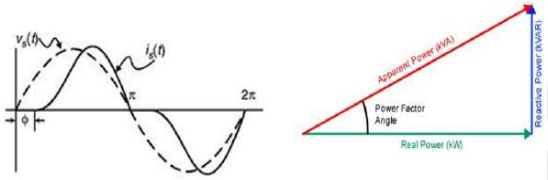

FIG. 4: (a)VOLTAGE AND DISTORTED LINE CURRENT WAVE FORM & (b) POWER TRIANGLE

As shown in equation 3, for a given power P, current I taken by load changes inversely with load power factor. As a result, a given load draws more current with a low power factor, increasing copper losses and lowering system efficiency. Three-phase induction motors, transformers, and lighting are the loads responsible for the low PF. The active kind of power factor correction circuit depicted in Fig. 5 is used to increase power factor by modifying the waveform of current taken by a load. Active PFCs include synchronous condenser, buck, boost, & buck-boost converters.

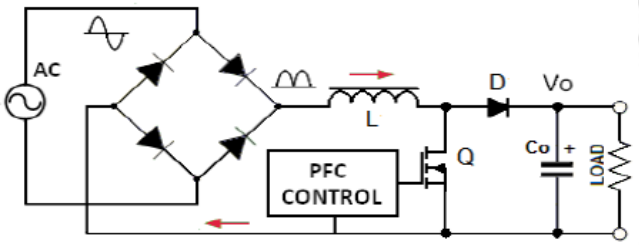

FIG. 5: PFC CIRCUIT

A perfect Power Factor Correction (PFC) would be one that follows a resistor on the source side while maintaining a sufficiently synchronised response potential difference. The converter must obtain a sinusoidal current from service in case of sinusoidal phase voltage. The primary goal of PFC procedure is to reduce reactive power and get the power factor closer to one. In this case, low power factor is caused by inductive loads, which may be remedied by inserting electrical devices such as capacitors into circuit. Commercially, there are several PFC machines available to collect different types of conditions. Fixed PFC is used when the power factor is low and no single piece of equipment is solely responsible (A. Consoli, 2001, Reinert J, Schroder S. (2002). In this state, the PFC capacitors and capacitor bank terminals are connected to each three phase wire for power factor correction. At this time, PFC can be connected to the switchgear. Yet, there are other circumstances in which PFC is not so straightforward. When various machines switch on and off repeatedly, the power factor may be modified to account for the changes in the system. In these circumstances, requisite PFC capacitors must be mechanically regulated, that is, banks of capacitors must be correctly switched in & out of power network. To stimulate which form of sluggish power converter is most recommended for a given application, several problems, such as robustness, power compactness, effectiveness, price, & difficulty, must be in use to the point. Under this subject, several converter topologies such as buck, boost, and cuk converter topologies have been proposed in recent years (Najmeh Zamani; 2914-Saijun Zhang; 2014) with the goal of improving the individuality of standard converters used for power factor.

The contemporary power factor correction process with PWM rectifier & Buck- Boost converter is commonly advised to give compensated currents similar to harmonic currents formed by nonlinear loads. These results reduce filter's value, & no specific dedicated power devices are required for harmonic mitigation. A PI control is used to follow necessary line current instruction, displaying single-phase diode rectifier coupled with these converters, which is widely used inactive PFC. In addition to geometric properties mentioned above, the buck-boost topology is too basic & accepts low-distorted source currents with about unity power factor using multiple dedicated governor procedures such as hysteresis control and PI control techniques.

OBJECTIVES OF THE STUDY

1. To simulate a closed-loop controlled power factor correction converter feeding a PMBLDC motor drive using buck-boost converters.

LITERATURE REVIEW

Ashmore et al. (2015) developed a solar support assembly in which the horizontal frame is coupled to a single pivotal point, resulting in inclination (sag) of the horizontal frame on both frame ends. As a result of the Center's sole support, the seasonal drive arrangement may not operate effectively.

Todd Griffith et al. (2015) offer structural dynamics testing & analysis for heliostat design assessment & monitoring. Vibrations, strain, & displacements under

International Journal on Recent and Innovation Trends in Computing and Communication
ISSN: 2321-8169 Volume: 11 Issue: 8
***Article Received:** 20 may 2023 **Revised:** 28 May 2023 **Accepted:** 16 August 2023*

wind loading are measurement parameters. This data aided in the evaluation and strengthening of structural models that anticipate system deformations owing to static gravity and dynamic wind loadings. It was discovered that optical precision is greatly influenced.

Eldin et al. (2016) stated that the employed mathematical model was experimentally confirmed and then applied to many conditions, notably hot & cold locations. In the case of a chilly city like Berlin, Germany, gain in electrical energy by following the Sun is roughly 39 percent. Due to over heating of PV panels, energy gain does not surpass eight percent in such a hot city like Aswan, Egypt. Nevertheless, if the energy necessary to run the monitoring device is included in this study, which varies from 5% to 10% of the energy generated, then tracking the Sun will be impossible in warmer nations. Only real-time implementation results can help you make the best selection.

Singh et al. (2016) demonstrate a dual output PFC converter for driving switching reluctance motors (SRMs). In this case, a modified SEPIC converter is employed for wide-range speed control and power factor correction at AC mains. A single voltage sensor is utilised to manage DC link voltage, and its output is used to drive midpoint converter feed SRM. To lower overall size of converter, switching frequency of converter is set at twenty kHz. It also discusses the general design & performance of converter-fed SRM drive. According to the IEC 6100-3-2 standard, the input current THD (Total Harmonic Distortion) is kept below 5%.

Wang et al. (2017) create a SEPIC using a half-bridge LLC resonant converter. This architecture lowers system costs while increasing dependability. Switching losses are minimised because the LLC resonant component retains soft switching characteristics. System bus voltage may be maintained low in high-power LED driving systems by carefully selecting characteristics. To validate theoretical analysis, certain tests with a 100-W prototype are carried out. The obtained power factor was as high as 0.99, & the efficiency is up to 92% at full load due to soft-switching operations.

Muntasir Alam et al. (2017) suggested a PWM-controlled hybrid resonant bridgeless AC-DC Power Factor Correction (PFC) boost converter. The proposed Paru Co., Ltd Korea 2018, PARU Technology Dual Axis Tracker (PST-2AL) has a surface size of 85 m2 with 49 modules of cells mounted in the surface area. Without modules, the structure weighs 1970 kg. The system's disadvantage is that it is not feasible to raise the longitudinal, and the rated power of the azimuth slewing motor is high.

Junming Zhang (2017) suggested a hybrid PFC converter with low output voltage & continuous input current by merging step-up PFC and step-down (Buck) PFC converters. The author has designed an improved peak current control technique that enables universal input range; a 150-W prototype has also been created and theoretically validated.

Jayachandran et al. (2017) introduce an air conditioning One Cycle Controlled (OCC) Bridge-less (BL) SEPIC converter fed Brush-Less DC (BLDC) motor drive. Its drive's speed is controlled by a 3-phase Voltage Source Inverter using Pulse Amplitude Modulation (PAM) (VSI). The DC bus voltage fluctuation through duty ratio modulation of BL-SEPIC converter switches facilitates pulse amplitude modification. To manage duty ratio of BL-SEPIC converter, a nonlinear approach known as One Cycle Control (OCC) is utilised. Auto shaping of supply current is accomplished by constructing a BL-SEPIC converter to operate in Discontinuous Inductor Current Mode (DICM). The Total Harmonic Distortion (THD) of supply current is kept within IEC-61000-3-2 limitations.

V. Viswanathan and Jeevananthan Seenithangom (2018) suggested a SEPIC converter with high static gain & low switching voltage stress; moreover, the converter is employed for torque ripple. In BLDC drive, the authors employed a three-level NPC inverter. The suggested SEPIC converter is not used to increase power factor.

Zhang et al. (2019) designed and analysed the double-axis gadget (mechanical structure). The Finite Element Method was used to generate parameterized model (FEM). The static analysis was performed to determine the displacement and stress distributions, as well as the stress evaluation, which was performed under various operating situations. The start-up of fulfilling the stress intensity, the lightweight, was completed, and this served as the foundation for the device's prototype test. This study covers improved design working procedures that were carried out using a mathematical model, generated the Finite Element Model (FEM), applied the boundary conditions, and calculated and evaluated the stress. The prototype model's tracking precision is a bit greater, and the full load of the moving structure is in two key locations, which may lead to failure at times.

Nasir, Ab-Kadir, and co. (2019) PV panels are particularly susceptible to direct & indirect lightning, as well as other surge over voltages, and the proper rating of Surge Protection Device (SPD) must be fitted to prevent electrical system damage. The suggested solar tracker system includes a device of type II class (lightning + surge voltage protection).

Lim and colleagues (2020) developed a large-scale dual-axis solar monitoring system that incorporates many

International Journal on Recent and Innovation Trends in Computing and Communication
ISSN: 2321-8169 Volume: 11 Issue: 8
***Article Received:** 20 may 2023 **Revised:** 28 May 2023 **Accepted:** 16 August 2023*

row elevation structures as well as a vertical-axis rotating platform. The installation has a power of 60 kWp, a diameter of 35 m, and a transmission system that turns the whole rotating platform. The transmission mechanism is made up of an AC motor (750 WAC) with a gearbox, 22 DC motors (15 WDC) for elevation motions, cylindrical pins, & a double layerpin-gear, all of which are unique design concepts that have been applied in a large-scale dual axis tracking system. The energy converter does away with the need for a diode bridge rectifier at the front end. Because the switches share the PWM gating signal, there is no need for additional circuitry to detect positive or negative ac input. The author created a 650-W prototype with a switching frequency of 70 kHz and a 400-volt alternating current output voltage.

Nasib Khadka, Aayush Bista, and colleagues (2020) describe numerous cleaning technologies that have been created and are still in use today. In the suggested method, manual cleaning is performed once a month using water wash.

William Cai et al. (2021) provide a summary of current research and technological advances in electric motor systems & electric power trains for new energy vehicles. Permanent magnet synchronous motors offer improved overall performance when compared to converters with Si-based IGBTs; converters with SiC MOSFETs have much higher efficiency & enhance driving mileage percharge when compared to converters with Si-based IGBTs. Moreover, the benefits and drawbacks of various control methods and algorithms are discussed. Finally, a technological roadmap for the next 15 years is offered, including the critical materials and components for the traction motor, power electronic converter, & electric power train for each time frame.

Maksim Sitnikov et al. (2021) study the major techniques of boosting the efficiency of electromechanical converters as well as new types of materials utilised in such devices. The economic ramifications and causes for the shift to extremely energy efficient electrical machines, as well as the introduction of special electrical machines in serial and mass manufacturing, are given specific consideration.

T M Khalina (2022) investigate a novel semiconductor device for starting a 3-phase induction motor from a single-phase network. Researchers were able to analyse the electromechanical properties of an induction motor when powered by a single-phase network using device simulation model created in Matlab Simulink environment. The parameters of motor during operation are compared using a 3-phase & a single-phase network. The investigation's findings indicate that developed gadget may be used to start & run a squirrel cage induction motor from a single-phase network. Simultaneously, engine's energy characteristics change somewhat.

PFC BUCK-BOOST CONVERTER FED PMBLDC MOTOR

Single stage PFC circuits are currently experiencing significant hurdles in order to boost output power capabilities with optimal component ratings. A conduction-mode buck-boost PFC converter with anon-inverting dc output has been proposed for wide input voltage range applications. This chapter is about digitally simulating a Power Factor Correction (PFC) buck boost converter for variable speed driving using a PMBLDC motor. The PFC is used in conjunction with a single-phase AC-DC converter architecture, which is then followed by a buck-boost bridge converter. A PI controller controls the DC link voltage, which is proportional to the desired speed of the PMBLDC motor, to accomplish speed control.

This paper describes the average current control strategy for the cascaded buck-boost converter using two loops connected to the buck boost converter. The power factor of the circuit is improved by comparing the input current with a sinusoidal current reference in the inner current loop, and the output voltage is controlled by the outer loop. Its drive ensures better power factor, excellent precision, stable operation, and increased efficiency. The PFC converter has non-inverted DC output voltage and can work in both step-up and step-down modes. The suggested topology is capable of working in both continuous and discontinuous conduction modes for high-power applications. A larger power factor may be attained over a wide range of output voltage by employing a buck boost converter. There are two working modes in a buck-boost converter that allow both step-up and step-down voltage conversion based on the operation of the switches, namely buck, boost, and buck-boost modes. The suggested technology, which combines buck and boost modes in a single power stage, provides an easy way to achieve unity power factor for an AC/DC converter.

MATHEMATICAL MODEL OF THE PFC BUCK-BOOST CONVERTER

Figure 6 depicts a proposed buck-boost converter, which is an uncontrolled diode bridge followed by a Buck-Boost Converter (BBC) with the storage elements Capacitor C with voltage c V, inductor L with current L I output voltage Vo, Supply voltage E, output current Io, magnitude current Im, power switch S, and load resistance R. Based on the duty ratio 'd,' the converter provides an output voltage

International Journal on Recent and Innovation Trends in Computing and Communication
ISSN: 2321-8169 Volume: 11 Issue: 8
Article Received: *20 may 2023* ***Revised:*** *28 May 2023* ***Accepted:*** *16 August 2023*

that is more or less than the input voltage. When switch S is turned on, the inductor current L I rises and diode D fails to conduct. When the switch S is turned off, the inductor current flows through the diode.

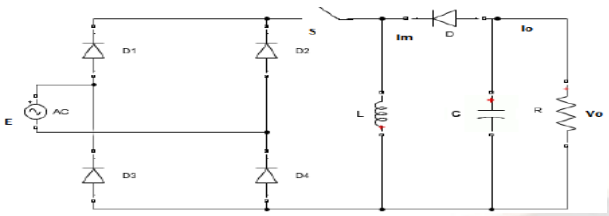

FIGURE 6 PFC BUCK BOOST CONVERTER TOPOLOGY

State-space models provide a broad and solid foundation for dynamic modelling of diverse systems, including power converters. State space models may be used to create linear control loops and mimic steady-state and dynamic behaviour using feedback control loops. The buck-boost converter's voltage transfer gain is

$$\frac{V_0}{E} = -\frac{d}{(1-d)} \quad (4)$$

The corresponding current transfer gain is

$$\frac{I_0}{I_m} = \frac{(1-d)}{d} \quad (5)$$

The switch conducts and the diode does not conduct in the on-duration circuit setup. Equations 4.9 exhibit state equations indicating the on-interval circuit setup.

$$\frac{di_L}{dt} = \frac{E}{L} \quad (6)$$

$$\frac{dV_c}{dt} = -\frac{1}{RC}V_c \quad (7)$$

$$\begin{bmatrix} \frac{di_L}{dt} \\ \frac{dV_c}{dt} \end{bmatrix} = \begin{bmatrix} 0 & 0 \\ 0 & \frac{-1}{RC} \end{bmatrix} \begin{bmatrix} i_L \\ V_C \end{bmatrix} + \begin{bmatrix} \frac{1}{L} \\ 0 \end{bmatrix} E \quad (8)$$

The switch opens and the diode conducts in the off-duration circuit setup. The off-circuit topology's state equations are provided as

$$\frac{di_L}{dt} = -\frac{V_c}{L} \quad (9)$$

$$\frac{dV_c}{dt} = \frac{1}{C}i_L - \frac{1}{RC}V_c \quad (10)$$

$$\begin{bmatrix} \frac{di_L}{dt} \\ \frac{dV_c}{dt} \end{bmatrix} = \begin{bmatrix} 0 & \frac{-1}{L} \\ \frac{1}{C} & \frac{-1}{RC} \end{bmatrix} \begin{bmatrix} i_L \\ V_c \end{bmatrix} \quad (11)$$

Using the state space averaging model the system model is written as

$$\begin{bmatrix} \frac{di_L}{dt} \\ \frac{dV_c}{dt} \end{bmatrix} = \begin{bmatrix} 0 & -\frac{1+d}{L} \\ \frac{1-d}{C} & \frac{-1}{RC} \end{bmatrix} \begin{bmatrix} i_L \\ V_C \end{bmatrix} + \begin{bmatrix} \frac{1}{L} \\ 0 \end{bmatrix} E \quad (12)$$

SIMULATION RESULTS

MATLAB simulation was performed using the intended circuit parameters, and the results are provided below. The magnitude of the reference speed was set to 1800 rpm, and the load torque was varied at time t=1 sec. Buck-boost converters Figure 7 depicts a Simulink model. Figure 8 depicts the Simulink model of a closed loop controlled PMBLDC motor with a PFC buck boost converter and a PI controller. To enhance the power factor, a buck boost converter is employed at the input. Figure 9 depicts the AC input voltage and current waveforms. Figure 10 depicts the step change in load torque.

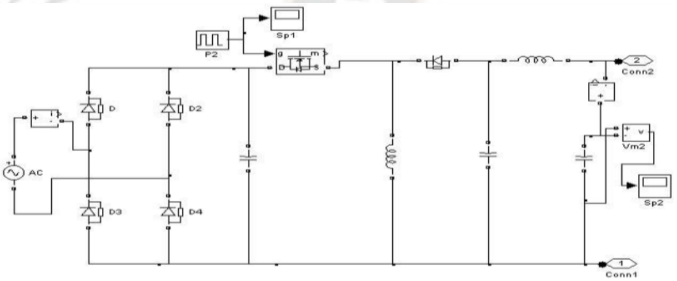

FIGURE 7 BUCK-BOOST CONVERTER

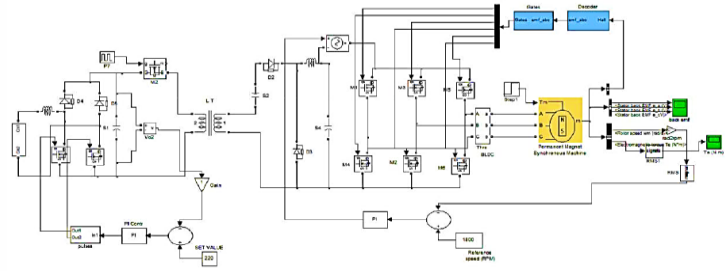

FIGURE 8: CLOSED LOOP SPEED CONTROL OF THE PMBLDC MOTOR WITH PFC BUCK-BOOST CONVERTER

International Journal on Recent and Innovation Trends in Computing and Communication
ISSN: 2321-8169 Volume: 11 Issue: 8
Article Received: *20 may 2023* ***Revised:*** *28 May 2023* ***Accepted:*** *16 August 2023*

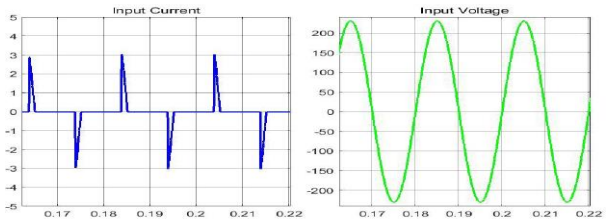

FIGURE 9: INPUT VOLTAGE AND CURRENT WAVEFORMS

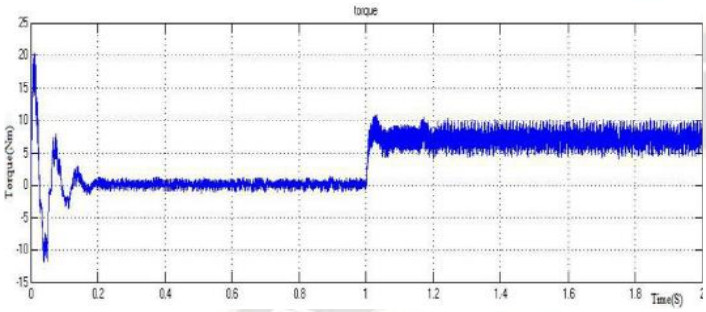

FIGURE 10: STEP CHANGE IN THE LOAD TORQUE APPLIED AT T=1 SEC

The closed loop mechanism returns the speed to normal and keeps it steady even throughout the load torque. The speed of the PMBLDC motor is maintained constant, as shown in Figure 11. The THD is only 4.71%, according to the FFT analysis in Figure 12, but the power factor is greater with the buck-boost converter fed PMBLDC drive, and it is higher than with the PFC bridgeless boost converter fed PMBLDC drive.

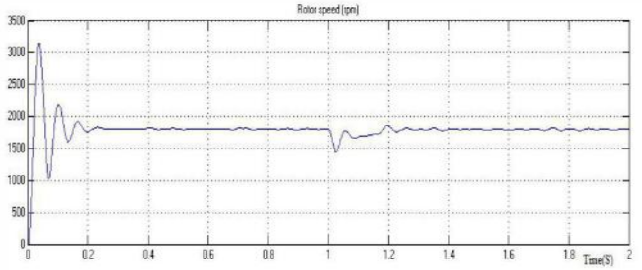

FIGURE 11 SPEED RESPONSE CURVE

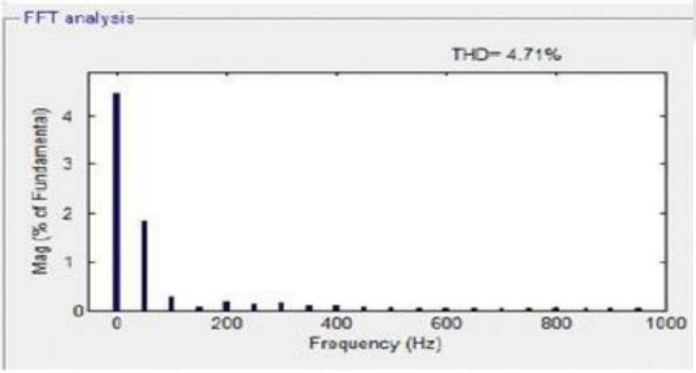

FIGURE 12 THD OF THE SOURCE CURRENT

EXPERIMENTAL RESULTS

As a hardware prototype, the buck-boost converter fed PMBLDC motor drive was constructed. Figure 13 depicts the hardware from the top. A buck boost converter and inverter circuits, a control circuit, and the PMBLDC motor compose the hardware prototype. Figure 14 depicts the experimental setup. Figure 15 depicts the input voltage and current waveforms. Figure 16 depicts the harmonic spectrum of the source voltage.

The technical specifications of the drive system are as follows: L = 150 mH, C = 220 μF, R= 5 . the bridgeless boost converter fed by 48v dc and the output is 58V .Other components are: Diode IN4007, Microcontroller AT89C2051, MOSFET IRF840, Driver IR2110, Voltage (0-500V) and Current is 8A.

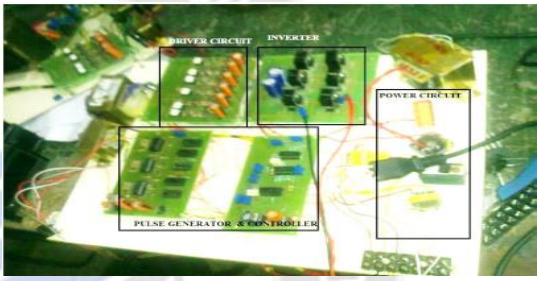

FIGURE 13 TOP VIEW OF THE HARDWARE

FIGURE 14 EXPERIMENTAL SETUP

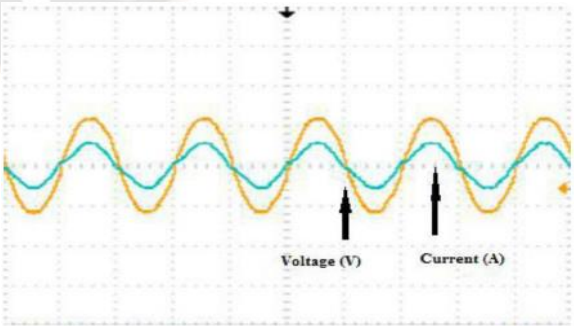

FIGURE 15 VOLTAGE AND CURRENT WAVEFORMS

International Journal on Recent and Innovation Trends in Computing and Communication
ISSN: 2321-8169 Volume: 11 Issue: 8
***Article Received:** 20 may 2023 **Revised:** 28 May 2023 **Accepted:** 16 August 2023*

FIGURE 16: HARMONIC SPECTRUM OF THE SOURCE VOLTAGE

Because the popular boost converter's main condition is that the output voltage be greater than the input voltage, its uses are restricted. A buck-boost converter can achieve a greater power factor across a wide range of output voltage.

CONCLUSION

In this research, the induction motor and BLDC motor drives were examined using buck boost converters which were simulated and implemented in hardware prototypes. Matlab/simulink was used to model the boost converter with compound active clamping and FSTPI fed induction motor driving. To reduce the resonance in winding inductance and junction capacitance, the boost converter with compound active clamping supplied IM drive requires an extra diode and inductor. The planned converter was executed with an FSTPI fed induction motor, and results were obtained. The simulation of a PFC buck-boost converter-based PMBLDC motor drive is compared to the experimental findings. Using a PI controller, the driving signals for the inverter switches are obtained from the feedback signals from the PMBLDC motor, which indicate the speed and position. The hardware was made and tested. The use of the buck-boost converter has raised the power factor, resulting in increased efficiency.

REFERENCES

2. Leonhard W (2001) “Control of Electrical Drives”, 3rd ed., 470 pp., 2001, Springer-Verlag, Berlin, Germany.
3. Crowder R., (2006) Electric Drives and Electromechanical Systems, 308 pp., Elsevier, Oxford, UK, 2006.
4. A. Consoli, (2001)“Unipolar converter for Switched reluctance motor drives with power factor Improvement”. Sixteenth annual IEEE applied power electronics conference and exposition, vol.2, pp. 1103 – 1108, 2001.
5. Reinert J, Schroder S. (2002) Power-factor correction for switched reluctance drives. IEEE Transactions on Industrial Electronics. 2002;49(1):54–57. DOI: 10.1109/41.982248.
6. Najmeh Zamani; (2914) “ Bifurcation and chaos control in power-factor-correction boost converter” 2014 22nd Iranian Conference on Electrical Engineering (ICEE), 2014, Pages: 1307 - 1312, DOI: 10.1109/IranianCEE.2014.6999736.
7. Ashmore, E ' Modular solar support assembly', U.S Patent No. 9134045. 15 Sep. 2015.
8. Griffith, DT, Moya, AC, Ho, CK & Hunter, PS 2015, 'Structural dynamics testing and analysis for design evaluation and monitoring of heliostats', Journal of Solar Energy Engineering, Transactions of the ASME, vol. 137, no. 2.
9. Eldin, SAS, Abd-Elhady, MS & Kandil, HA 2016, 'Feasibility of solar tracking systems for PV panels in hot and cold regions', Renewable Energy, vol. 85, pp. 228-233.
10. Singh, et al. (2016) "Power Factor Correction in single-ended primary inductance converter fed switched reluctance motor drive‖, IEEE International Conference on Power Electronics, Intelligent Control and Energy Systems (ICPEICES), pp. 1-6, 2016.
11. Wang, Y, A single-stage LED driver based on SEPIC and LLC circuits‖, IEEE Transactions on Industrial Electronics, Vol. 64, No. 7, pp. 5766 5776, 2017.
12. Alam, M., Eberle, W., Gautam, D.S., Botting, C., Dohmeier, N. and Musavi, F., 2017. A hybrid resonant pulse-width modulation bridgeless AC–DC power factor correction converter. IEEE Transactions on Industry Applications, vol. 53 no.2, pp.1406-1415.
13. Zhang, J., Zhao, C., Zhao, S. and Wu, X., 2017. A family of single phase hybrid step-down PFC converters. IEEE Transactions on Power Electronics, vol. 32, no.7, pp.5271-5281.
14. Viswanathan, V. and Seenithangom, J., 2018. Commutation Torque Ripple Reduction in the BLDC Motor Using Modified SEPIC and Three-Level NPC Inverter. IEEE Transactions On Power Electronics, vol. 33 no.1, pp.535-546.
15. Zhang, S. Li, C, Zhang, J, Miao, H & Zhang, Y 2019, 'Design and structural analysis of the Sun ray

double axis tracking device', Journal of Solar Energy Engineering, vol. 141, ho. 4.

16. Nasir, MSM, Ab-Kadir, MZA, Radzi, MAM, Izadi, M, Ahmad, NI & Zaini, NH 2019, Lightning performance analysis of a rooftop grid- connected solar photovoltaic without external lightning protection system', Plos one, vol. 14, no. 7, pp. e0219326.
17. William Cai et al. (2021) "Review and Development of Electric Motor Systems and Electric Powertrains for New Energy Vehicles" Published: 25 February 2021 valum 4, pages3–22.
18. Maksim Sitnikov et al. (2021) "Trends and New Challenges in the Energy Efficiency of Electric Machines" Advances in Engineering Research, volume 213.
19. T M Khalina et al. (2022) "The development of an energy efficient electric drive for agricultural machines" Volume 1211, IXX International Scientific and Practical DOI 10.1088/1757-899X/1211/1/012018.